

# **Implementation of Nodal Equivalence Parameters in DIF3D-VARIANT for Core Analysis of Prismatic Very High Temperature Reactor (VHTR)**

---

**Nuclear Engineering Division**

**About Argonne National Laboratory**

Argonne is a U.S. Department of Energy laboratory managed by UChicago Argonne, LLC under contract DE-AC02-06CH11357. The Laboratory's main facility is outside Chicago, at 9700 South Cass Avenue, Argonne, Illinois 60439. For information about Argonne, see [www.anl.gov](http://www.anl.gov).

**Availability of This Report**

This report is available, at no cost, at <http://www.osti.gov/bridge>. It is also available on paper to the U.S. Department of Energy and its contractors, for a processing fee, from:

U.S. Department of Energy

Office of Scientific and Technical Information

P.O. Box 62

Oak Ridge, TN 37831-0062

phone (865) 576-8401

fax (865) 576-5728

[reports@adonis.osti.gov](mailto:reports@adonis.osti.gov)

**Disclaimer**

This report was prepared as an account of work sponsored by an agency of the United States Government. Neither the United States Government nor any agency thereof, nor UChicago Argonne, LLC, nor any of their employees or officers, makes any warranty, express or implied, or assumes any legal liability or responsibility for the accuracy, completeness, or usefulness of any information, apparatus, product, or process disclosed, or represents that its use would not infringe privately owned rights. Reference herein to any specific commercial product, process, or service by trade name, trademark, manufacturer, or otherwise, does not necessarily constitute or imply its endorsement, recommendation, or favoring by the United States Government or any agency thereof. The views and opinions of document authors expressed herein do not necessarily state or reflect those of the United States Government or any agency thereof, Argonne National Laboratory, or UChicago Argonne, LLC.

# Implementation of Nodal Equivalence Parameters in DIF3D-VARIANT for Core Analysis of Prismatic Very High Temperature Reactor (VHTR)

---

by  
C. H. Lee, H. K. Joo\*, W. S. Yang, and T. A. Taiwo  
Nuclear Engineering Division, Argonne National Laboratory

\* H. K. Joo is a visiting researcher from KAERI (ROK).

March 15, 2007

work sponsored by

U. S. Department of Energy,  
Office of Nuclear Energy, Science and Technology



UChicago ►  
Argonne<sub>LLC</sub>





## TABLE OF CONTENTS

	Page
TABLE OF CONTENTS .....	2
LIST OF TABLES .....	3
LIST OF FIGURES.....	4
ABSTRACT.....	5
1.0 INTRODUCTION.....	6
2.0 IMPLEMENTATION OF DISCONTINUITY FACTORS .....	7
3.0 VERIFICATION TESTS .....	9
3.1 Cross Section Generation.....	9
3.2 Two-Dimensional Core Calculations.....	12
4.0 CONCLUSIONS.....	19
REFERENCES .....	20

## LIST OF TABLES

	Page
Table 1. Group Boundaries (eV) of Cross Sections from DRAGON and HELIOS. ....	12
Table 2. Differences between MCNP4C and DRAGON/DIF3D Multiplication Factor, Power, and Control Rod Worth for 2-D Cores. ....	14
Table 3. Differences between MCNP4C and HELIOS/DIF3D Multiplication Factor, Power, and Control Rod Worth for 2-D Cores. ....	16

## LIST OF FIGURES

	Page
Figure 1. Two-Dimensional Model for the Rodded Reflector Region. ....	10
Figure 2. Two-Dimensional Models for the Rodded Fuel Region.....	11
Figure 3. Two-Dimensional Core Configuration with Control Rod Banks.....	13
Figure 4. Power Distributions from MCNP4C and DRAGON/DIF3D for 2-D Core with CA....	14
Figure 5. Power Distributions from MCNP4C and DRAGON/DIF3D for 2-D Core with CB and CA.....	15
Figure 6. Power Distributions from MCNP4C and DRAGON/DIF3D for 2-D Core with SA. ...	15
Figure 7. Power Distributions from MCNP4C and HELIOS/DIF3D for 2-D Core with CA.....	17
Figure 8. Power Distributions from MCNP4C and HELIOS/DIF3D for 2-D Core with CB. ....	17
Figure 9. Power Distributions from MCNP4C and HELIOS/DIF3D for 2-D Core with CA and CB.....	18
Figure 10. Power Distributions from MCNP4C and HELIOS/DIF3D for 2-D Core with SA. ....	18

## ABSTRACT

*The VARIANT module of the DIF3D code has been upgraded to utilize surface-dependent discontinuity factors. The performance of the new capability is verified using two-dimensional core cases with control rods in reflector and fuel blocks. Cross sections for VHTR components were generated using the DRAGON and HELIOS codes. For rodded block cross sections, the DRAGON calculations used a single-block model or the multi-block models combined with MCNP4C flux solutions, whereas the HELIOS calculations utilized multi-block models. Results from core calculations indicate that multiplication factor, block power, and control rod worth are significantly improved by using surface-dependent discontinuity factors.*

## 1.0 INTRODUCTION

In previous work, the REBUS-3/DIF3D code suite was modified in order to support the neutronics analysis of prismatic Very High Temperature Reactor (VHTR) cores. Two previous reports [1, 2] presented the enhancements to the DRAGON cross section generation approaches and the REBUS-3/DIF3D core analysis capabilities for the code suite. In Reference 2, it was discussed that the use of discontinuity factors not only reduced fuel block average power errors but also improved the core multiplication factor. In addition, it was observed that the nodal expansion method (NEM) option of DIF3D was not sufficiently accurate for an annular-type prismatic VHTR core and the VARIANT option of DIF3D provided a better spatial solution. [3, 4] It is noted that only the  $P_1$  approximation of the VARIANT option was used in order to utilize the nodal equivalence parameters. This is because VARIANT provides a nodal *transport* capability and equivalence parameters have typically been applied to the diffusion theory solution approaches.

The previous study also indicated that the core power tilt arising from asymmetrically rodded blocks could be improved by introducing surface-dependent discontinuity factors (DFs). The performance of surface-dependent DFs was shown at the mini-core level using the NEM option of DIF3D because the surface-dependent discontinuity factor capability was not available for the VARIANT option. Therefore, it was recommended that the capability be provided for that option.

In Section 2, the implementation of surface-dependent discontinuity factors into the VARIANT option of DIF3D is discussed. Section 3 summarizes cross section generation for VHTR components and discusses verification results from two-dimensional (2-D) core calculations. Conclusions from the work are given in Section 4.

## 2.0 IMPLEMENTATION OF DISCONTINUITY FACTORS

Discontinuity factors based on the nodal equivalence theory were previously implemented into the hexagonal diffusion theory option of the DIF3D code. Since the VARIANT module uses a within-group response matrix algorithm to solve for the partial current and reconstruct the flux moments, the same approach employed for the NEM module can be easily applied. Consequently, in this work, the same approach has been applied to the VARIANT option.

The main part of DIF3D influenced by DFs is the partial current-based response matrix equation. The form of the response matrix used in the VARIANT module is very similar to that in the NEM one:

$$J_g^+ = \mathbf{R}_g J_g^- + Q_g, \quad (1)$$

where,  $J_g^+$  = Outgoing current vector for group  $g$ ,

$J_g^-$  = Incoming current vector for group  $g$ ,

$\mathbf{R}_g$  = Response matrix for group  $g$ ,

$Q_g$  = Source moment vector for group  $g$ .

Before and after solving the response matrix equation in Eq. (1), the following simple transformation is applied to two partial currents at each surface:

$$\mathbf{A} J_g^{het} = J_g^{hom}, \quad \mathbf{A}^{-1} J_g^{hom} = J_g^{het}, \quad (2)$$

where  $J_g^{het}$  = Heterogeneous partial current vector for group  $g$ ,

$J_g^{hom}$  = Homogeneous partial current vector for group  $g$ ,

$$\mathbf{A} = \begin{bmatrix} \alpha & \alpha - 1 \\ \alpha - 1 & \alpha \end{bmatrix},$$

$$\alpha = \frac{f_g + 1}{2f_g}, \quad f_g = \frac{\phi_g^{het}}{\phi_g^{hom}}.$$

Instead of saving homogeneous partial currents, heterogeneous ones are saved in memory, and homogeneous partial currents are determined using Eq. (2) before solving the response matrix equation in Eq. (1). The homogeneous partial current solutions of the response matrix equation are then converted and saved back to the heterogeneous partial currents.

The importation of DF data from an external file is activated only when the NEM option is selected. Thus, it should also be activated for the VARIANT option. *Currently, however, a module was simply modified to read a temporary file of discontinuity factor data.* This should be completed in the future.

### **3.0 VERIFICATION TESTS**

The surface-dependent DF capability of the VARIANT option has been verified using 2-D core problems. In this section, cross section generation approaches for VHTR components such as fuel, reflector, and control rod (CR) will be recalled briefly and verification results with 2-D core models will then be discussed.

#### **3.1 Cross Section Generation**

The DRAGON [5] and HELIOS [6] lattice physics codes were used for cross section generation. The DRAGON code has a capability to model coated fuel particles explicitly at the assembly level but the multi-block modeling capability is limited. On the other hand, the HELIOS code has better capabilities for multi-block lattice calculations but cannot model particulate fuels explicitly.

Fuel block cross sections are generated using single block calculations with reflective boundary conditions, assuming that the neutron spectrum of the fuel block is primarily dependent on its own characteristics. Due to the geometry modeling limitation of the DRAGON code, the fuel-element handling hole in the center of the fuel block is approximated using two-ring hexagonal cells with the number density of graphite modified to preserve the graphite content of the fuel block.

Reflector cross sections significantly vary with distance from the interface between the core and reflector regions because the thermal neutron spectrum changes significantly at this interface. The application of discontinuity factors makes it possible to use a single-set of cross sections for each of the inner, outer, and axial reflector regions with good accuracy. A two-region (fuel-reflector) one-dimensional (1-D) model is used for generating the reflector cross sections. In the DRAGON calculation, the hexagonal pin-cell geometry is changed to a slab-cell maintaining the same fuel-to-moderator volume ratio; this is necessary because the DRAGON solution for the fuel-reflector problem with pin-cell geometry is not sufficiently accurate, compared to the MCNP reference results. Using the HELIOS code, the hexagonal pin-cell geometry is converted to rectangular pin-cell geometry for the 1-D model. Discontinuity factors at the interface between the fuel and reflector are calculated by dividing the heterogeneous

surface fluxes of the DRAGON solution by the homogeneous surface fluxes obtained from a finite difference method (FDM) solution.

Since the DRAGON code has geometry modeling limitation for multi-block calculations, a two-step *hybrid* procedure based on MCNP4C [7] solutions was introduced to determine rodded reflector cross sections. Specifically, region-wise average fluxes, surface fluxes, and currents are derived from MCNP4C solutions for a multi-block calculation (see Figure 1). The MCNP4C region-wise flux data are imported into DRAGON to calculate homogenized cross sections for the rodded reflector block. Using the homogenized cross sections from DRAGON and the boundary current sources from MCNP4C, a finite difference method (FDM) calculation is performed to solve for homogeneous surface fluxes. Discontinuity factors at the six surfaces of the rodded reflector block are determined dividing the homogeneous surface fluxes from the FDM solution by the heterogeneous surface fluxes from the MCNP4C solution. For the HELIOS calculations, the seven-block configuration is modeled directly without the support of MCNP4C solutions. The cylindrical control rod is approximately represented by three hexagonal-cell rings (in the plane) in the HELIOS calculations.

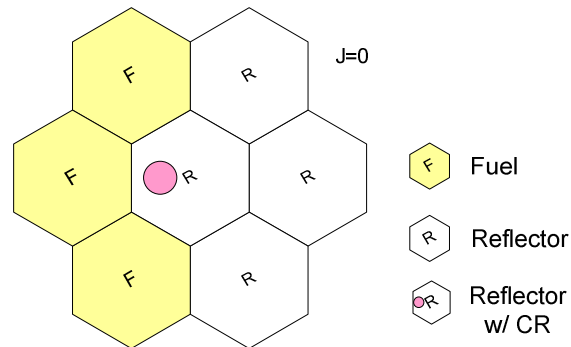


**Figure 1. Two-Dimensional Model for the Rodded Reflector Region.**

For a rodded fuel block in which a control rod is inserted in a sixth sector (see the middle assembly in Figure 1), DRAGON calculation utilizes a single-block model as for normal fuel blocks. The cylindrical control rod is approximated with three hexagonal-cell rings as shown in Figure 2(a). Six surface-dependent DFs are derived by simply dividing surface fluxes by block average fluxes. However, a preliminary study showed that the use of homogenized cross sections and DFs generated using a single-block model leads to a higher block power and lower control

rod worth compared to MCNP4C reference values. This is because the thermal flux depression in the rodded sector is exaggerated with the reflective boundary condition of the single block model, resulting in lower absorption cross sections. It is noted that the control rod pattern of the VHTR core does not have rodded sectors of neighboring blocks facing each other and hence the reflective boundary condition is inadequate. Therefore, it is imperative to use a multi-block calculation for a rodded fuel block, as shown in Figure 2(b), in order to obtain more realistic homogenized cross sections and equivalence parameters for rodded fuel blocks. As aforementioned, the DRAGON code has a limitation in establishing multi-blocks, and thus the HELIOS code is used for generating cross sections of rodded fuel blocks from the multi-block lattice calculation.

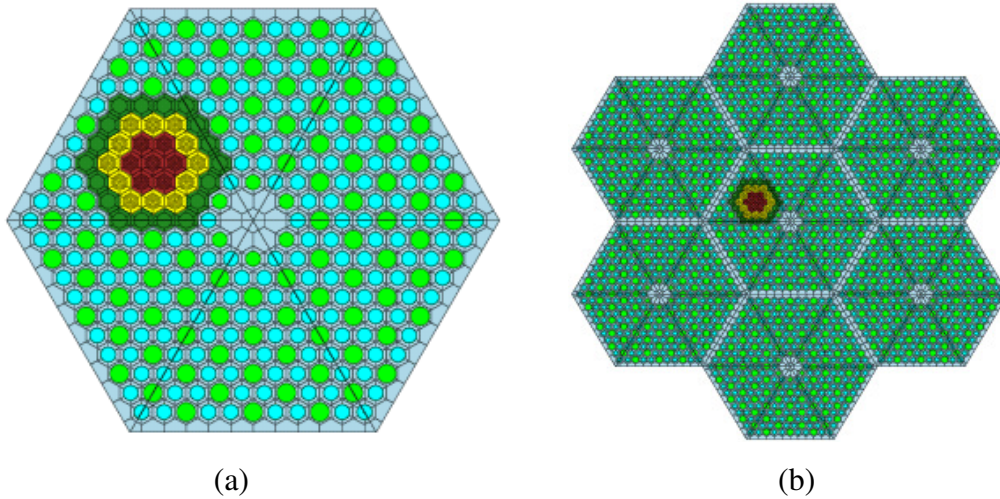


**Figure 2. Two-Dimensional Models for the Rodded Fuel Region.**

In DRAGON, the 172-group cross section library which was created by the Reduced Enrichment for Research and Test Reactor project is used in lattice calculations for generating 23-group cross sections, whereas for HELIOS, a 190-group cross section library is utilized for generating 20-group cross sections. The group structures are presented in Table 1. It is noted that all cross sections in this study are generated based on the homogeneous fuel compact model in order to eliminate the errors arising from the treatment of the double heterogeneity effect of TRISO fuel particles.

**Table 1. Group Boundaries (eV) of Cross Sections from DRAGON and HELIOS.**

DRAGON (23-group)		HELIOS (20-group)	
1.964E+7	0.972	2.000E+6	0.971
3.679E+6	0.850	3.679E+6	0.834
1.353E+6	0.500	1.353E+6	0.503
5.000E+5	0.400	4.979E+5	0.417
1.110E+5	0.350	1.111E+5	-
6.738E+4	0.300	-	0.301
9.118E+3	0.250	9.119E+3	-
3.673E+2	0.180	3.536E+2	0.184
4.000	0.140	3.928	0.146
1.500	0.100	1.525	0.112
1.097	0.050	1.099	0.050
1.045	1.1E-4	1.043	0.000

### 3.2 Two-Dimensional Core Calculations

Two-dimensional cores have been established to verify the surface-dependent discontinuity factor capability implemented into the VARIANT module of DIF3D. Since surface-dependent discontinuity factors are particularly useful for asymmetric blocks or configurations, the two-dimensional cores contain asymmetrically rodded fuel or reflector blocks. In prismatic VHTR cores, control rods are inserted in reflector blocks for regulating purposes during operation and in fuel blocks for startup or shutdown purposes. For simplicity, the locations of blocks with control rods are changed from the original VHTR design to give one-twelfth core symmetry. Figure 3 shows the locations of control rods in reflector and fuel regions for the cores: control rod banks CA and CB are inserted in the reflector region and safety rod bank SA in the fuel region. Four core configurations were established using different patterns of rodded blocks: cases with CA in, CB in, CA+CB in and SA in.

In the first set of verification tests, the cross sections were obtained from DRAGON calculations. The cross sections and discontinuity factors of rodded reflector block were determined using the MCNP4C solutions for a seven-block calculation, as discussed in Section 3.1. Those of the rodded fuel block were obtained from a single-block DRAGON calculation. Table 2 summarizes differences in core  $k_{\text{eff}}$  value, power and control rod worth between MCNP4C and DRAGON/DIF3D solutions.

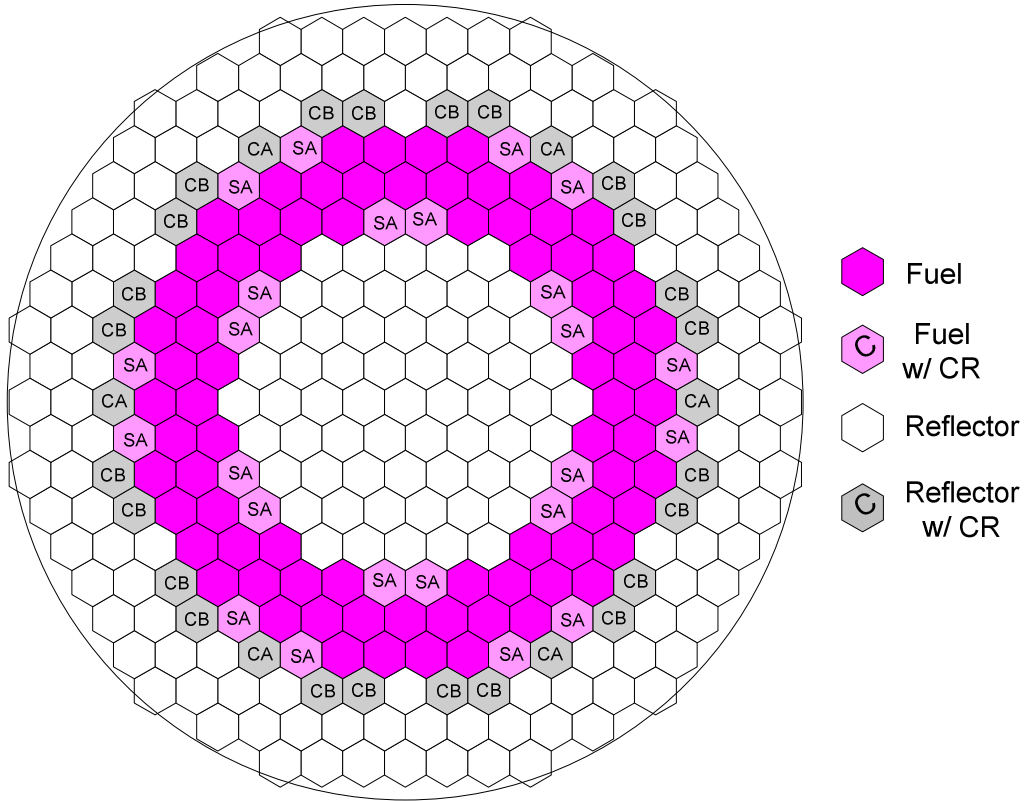


**Figure 3. Two-Dimensional Core Configuration with Control Rod Banks.**

Without DFs, large power errors occurred at the fuel blocks adjacent to the rodded blocks, as shown in Figures 3, 4, and 5. Errors in control rod worth and power of DRAGON/DIF3D solutions were reduced for all cases by using DFs. However, it is observed in Figures 4 and 5 that even after applying DFs, the magnitude of power errors is still large: 12.1 % and 12.6 % for the cases with CA+CB or SA, respectively. The large errors for the case with control rods CA+CB in the reflector region could be caused by inaccurate cross sections and equivalence parameters of the rodded reflector blocks obtained with 23-group region fluxes, surface currents and heterogeneous fluxes of MCNP4C solutions, which are subject to relatively large uncertainties. The errors for the case with safety rod bank SA in the fuel region are due to the single-block calculation with the reflective boundary condition, which is far from the real boundary condition. Therefore, it is necessary to use a multi-block model for generating rodded fuel block cross sections, in which a rodded fuel block is surrounded by unrodded fuel blocks.

**Table 2. Differences between MCNP4C and DRAGON/DIF3D Multiplication Factor, Power, and Control Rod Worth for 2-D Cores.**

Core Configuration		MCNP4C Eigenvalue <sup>a)</sup>	w/o DF			w/ DF		
			% $\Delta\rho$	Power, % (Max / RMS)	CR Worth, %	% $\Delta\rho$	Power, % (Max / RMS)	CR Worth, %
CR in Reflector	CA in	1.35799	0.261	9.7/3.4	-8.6	-0.136	3.3/1.4	-5.1
	CA+CB in	1.28223	0.141	18.9/8.1	-0.9	-0.361	12.1/4.8	1.9
CR in Fuel	SA in	1.22495	1.180	16.3/8.1	-10.9	0.295	12.6/4.5	-5.3

a) Standard deviation of MCNP4C results  $\leq 0.00036$

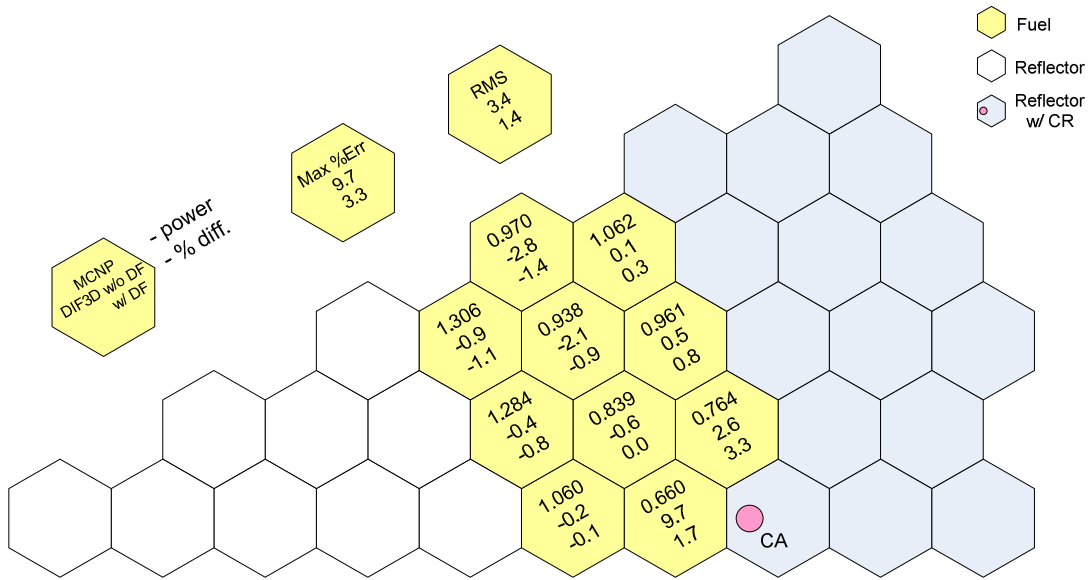


**Figure 4. Power Distributions from MCNP4C and DRAGON/DIF3D for 2-D Core with CA.**

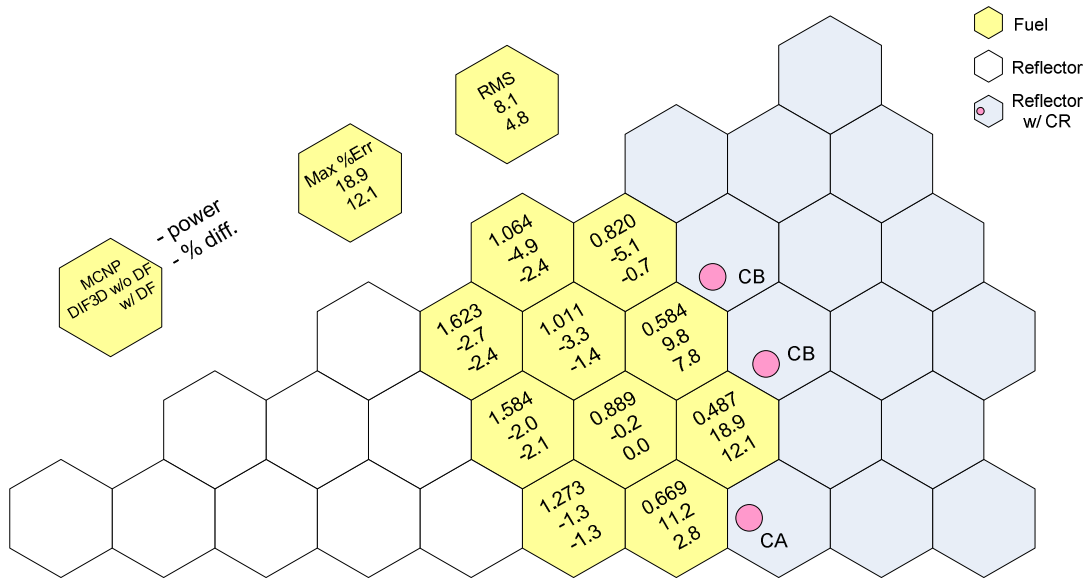


Figure 5. Power Distributions from MCNP4C and DRAGON/DIF3D for 2-D Core with CB and CA.

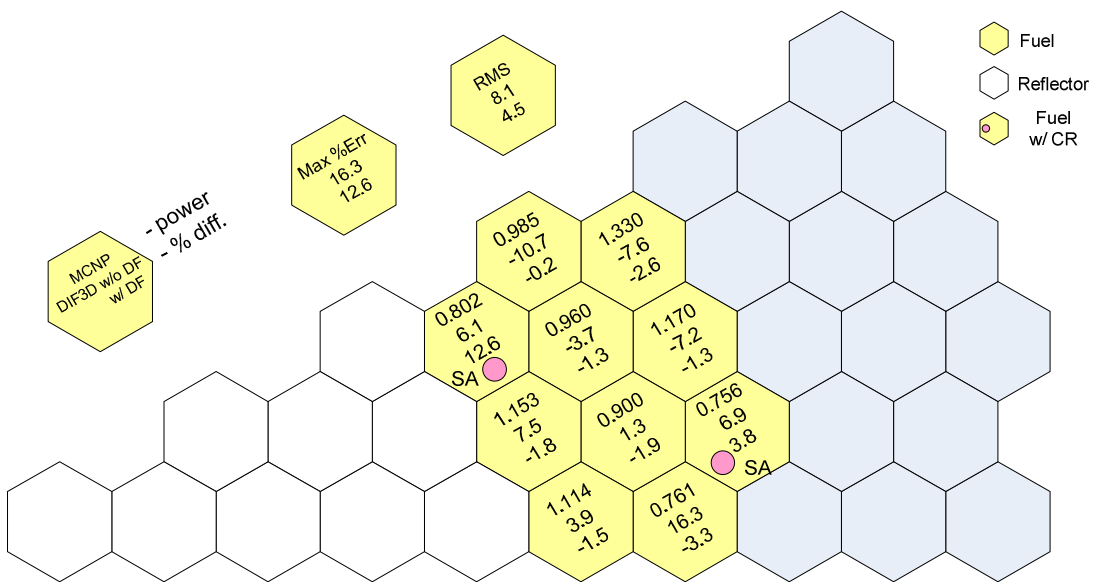


Figure 6. Power Distributions from MCNP4C and DRAGON/DIF3D for 2-D Core with SA.

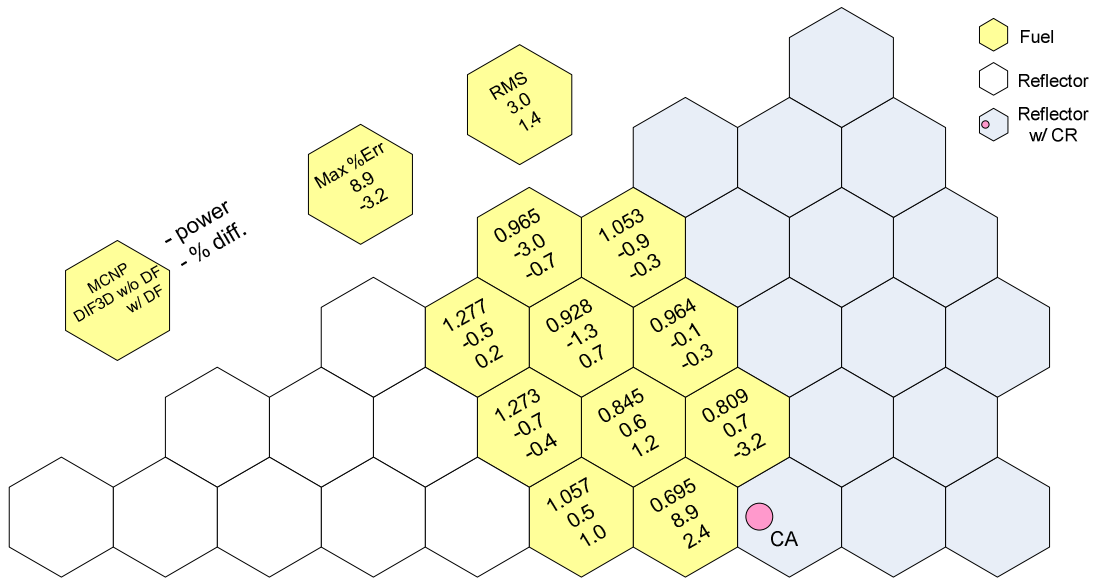
In the second set of verification tests, the cross sections were obtained from HELIOS calculations. As aforementioned, the HELIOS code is able to perform multi-block calculations for rodged fuel and reflector blocks. Since the cylindrical control rod is modeled with three hexagonal-cell rings, the MCNP4C model for the reference solution is changed accordingly (for consistency of comparison).

Table 3 is a summary of differences in multiplication factor, block power, and control rod worth between MCNP4C and HELIOS/DIF3D for 2-D cores with control rods. It is noted that the MCNP4C multiplication factors for the cases with control rods in the reflector region are different from those in Table 2 because of the change of control rod model. With the use of DFs, differences in control rod worth were substantially reduced, and maximum power errors were reduced to less than ~5 %. It is noted that the maximum percent power difference occurred at the fuel block with a low power. The detailed power distributions are presented in Figures 7 to 10. It can be seen by comparing control rod worths and power distributions of DRAGON/DIF3D and HELIOS/DIF3D results that rodged fuel block cross sections obtained from a multi-block model (HELIOS) give better results for the core reactivity and power distribution than those from a single block model (DRAGON).

**Table 3. Differences between MCNP4C and HELIOS/DIF3D Multiplication Factor, Power, and Control Rod Worth for 2-D Cores.**

Core Configuration		MCNP4C Eigenvalue <sup>a)</sup>	w/o DF			w/ DF		
			% $\Delta\rho$	Power, % (Max / RMS)	CR Worth, %	% $\Delta\rho$	Power, % (Max / RMS)	CR Worth, %
CR in Reflector	CA in	1.36657	0.215	8.9/3.0	-8.5	0.143	-3.2/1.4	-4.0
	CB in	1.31420	1.384	12.3/5.5	-29.9	0.387	-4.4/1.7	-6.8
	CA+CB in	1.29528	1.508	14.7/6.7	-25.4	0.637	5.3/2.3	-9.9
CR in Fuel	SA in	1.22495	1.610	12.9/7.0	-15.2	0.291	-4.7/2.1	-2.1

a) Standard deviation of MCNP4C results  $\leq 0.00037$



**Figure 7. Power Distributions from MCNP4C and HELIOS/DIF3D for 2-D Core with CA.**

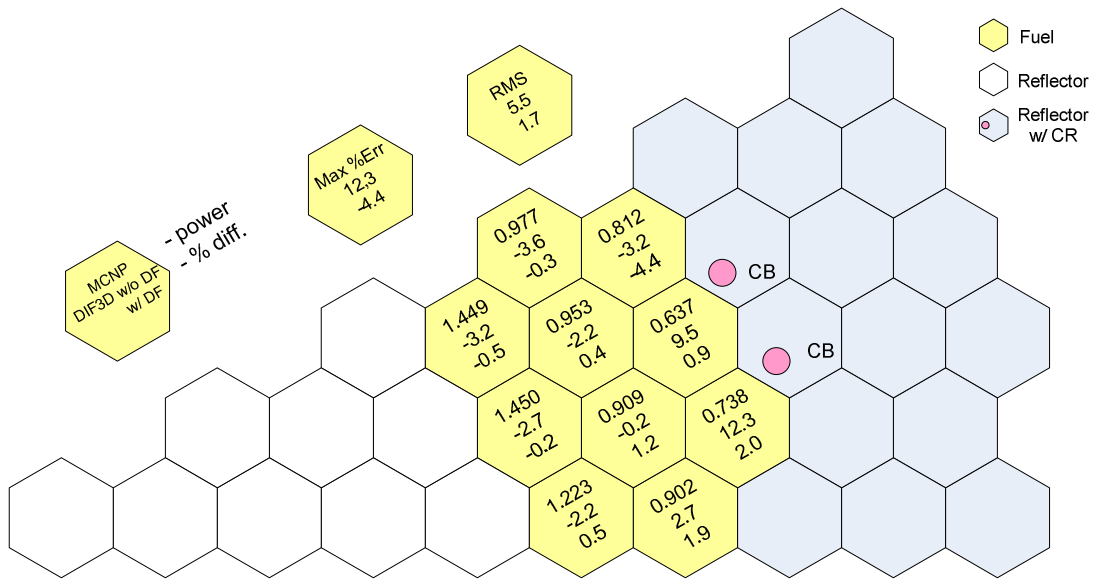


**Figure 8. Power Distributions from MCNP4C and HELIOS/DIF3D for 2-D Core with CB.**

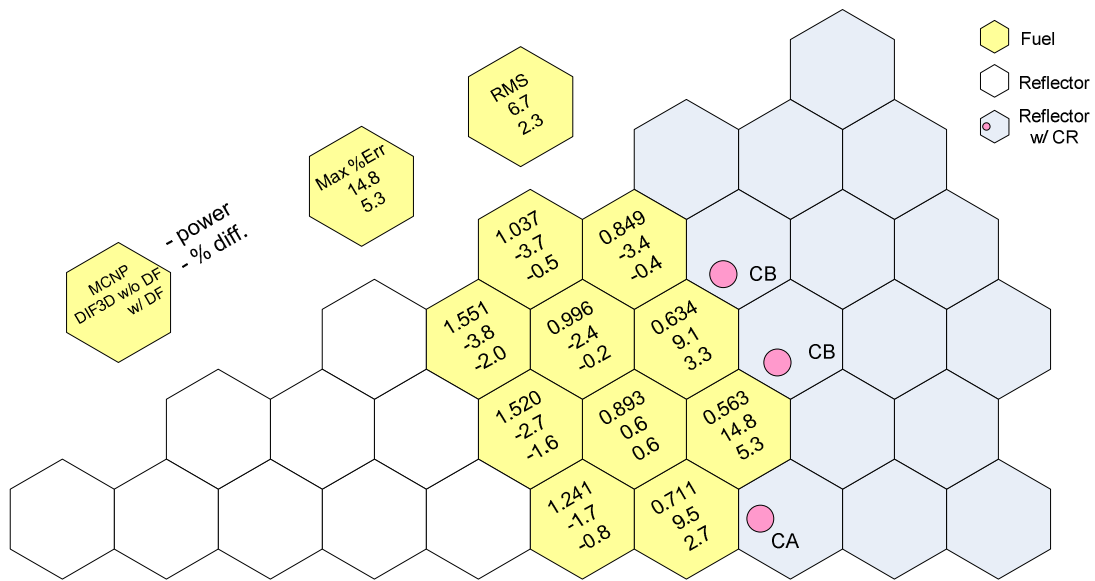


**Figure 9. Power Distributions from MCNP4C and HELIOS/DIF3D for 2-D Core with CA and CB.**

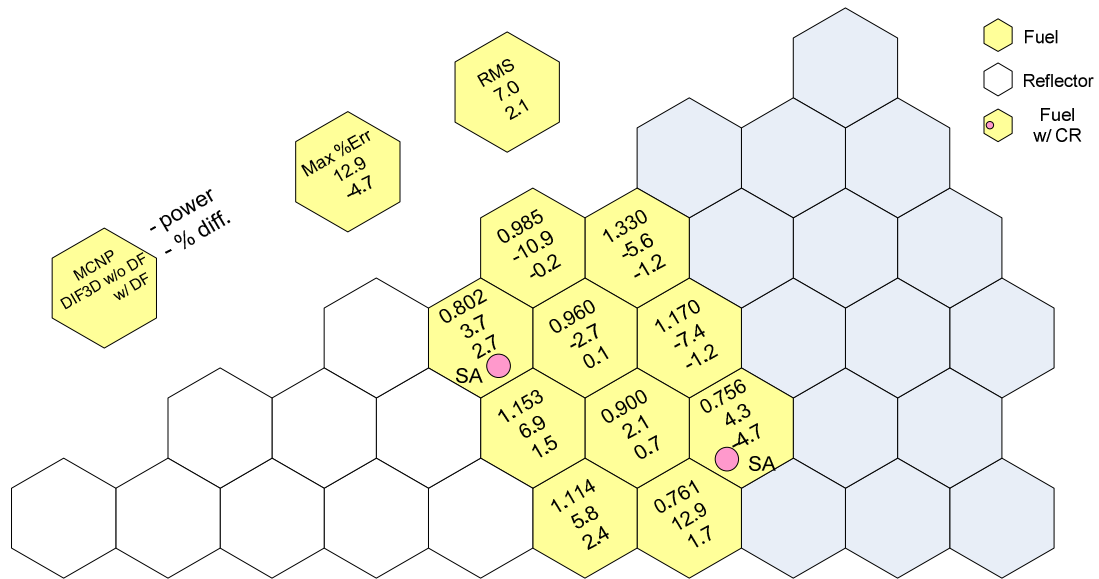


**Figure 10. Power Distributions from MCNP4C and HELIOS/DIF3D for 2-D Core with SA.**

## 4.0 CONCLUSIONS

Previous study has indicated that the nodal expansion method (NEM) option of DIF3D is not sufficiently accurate to simulate annular prismatic VHTR cores and that the  $P_1$  approximation of the VARIANT nodal transport option gives better results (due to improved spatial approximation) and should be used. Additionally, the asymmetric design for reflector or fuel blocks containing control rods required the use of surface-dependent discontinuity factors (DFs) to achieve good accuracy for the core multiplication factor and power distribution, when core calculations are performed based on one-node-per-hexagonal block. In this work, a surface-dependent DF capability has been added to the VARIANT module of DIF3D. The use of the new function (surface-dependent DFs) is limited to the  $P_1$  approximation of VARIANT, since this is consistent with previous practice in which DFs are applied with diffusion theory solutions.

The performance of the surface-dependent DFs has been verified using two-dimensional core models with control rods in reflector or fuel blocks. Cross sections for all VHTR components were generated using the DRAGON and HELIOS lattice codes, and core calculations were performed using the VARIANT option of DIF3D. Compared to MCNP4C solutions, DRAGON/DIF3D results indicated that core multiplication factor, block power, and control rod worth are significantly improved by using surface-dependent DFs, but still have large errors locally (low power blocks). The errors are attributed to inaccuracies arising from the single block or hybrid approach used for generating rodded block cross sections and equivalence parameters from DRAGON calculations. When the cross sections and equivalence parameters are generated with the HELIOS code, which allows the explicit modeling of a multi-block model configuration, the errors are significantly reduced. It was observed that the errors in core power distribution and control rod worth from HELIOS/DIF3D calculations are much smaller than those of DRAGON/DIF3D calculations. This indicates that in the future the DRAGON code should be modified to allow multi-block calculations.

## REFERENCES

1. C. H. Lee, Z. Zhong, T. Taiwo, W. Yang, M. Smith, and G. Palmiotti, "Status of Reactor Physics Activities on Cross Section Generation and Functionalization for the Prismatic Very High Temperature Reactor, and Development of Spatially-Heterogeneous Codes," **ANL-GenIV-075**, Argonne National Laboratory (2006).
2. C. H. Lee, Z. Zhong, T. Taiwo, W. Yang, H. S. Khalil and M. Smith, "Enhancement of REBUS-3/DIF3D for Whole-Core Neutronic Analysis of Prismatic Very High Temperature Reactor (VHTR)," **ANL-GenIV-076**, Argonne National Laboratory (2006).
3. R. D. Lawrence, "The DIF3D Nodal Neutronics Option for Two- and Three-Dimensional Diffusion Theory Calculations in Hexagonal Geometry," **ANL-83-1**, Argonne National Laboratory (1983).
4. G. Palmiotti, E. E. Lewis, and C. B. Carrico, "VARIANT: VARIational Anisotropic Nodal Transport for Multidimensional Cartesian and Hexagonal Geometry Calculation," **ANL-95/40**, Argonne National Laboratory (1995).
5. G. Marleau, et al, "A User Guide for DRAGON," Technical report **IGE-174 Rev. 4**, Ecole Polytechnique de Montréal, September 1998 (1998).
6. R. J. Stammli'er et al., "HELIOS Methods," Studsvik Scanpower (1998).
7. J. F. Briesmeister, Editor, "MCNP<sup>TM</sup> - A General Monte Carlo N-Particle Code, Version 4C," Los Alamos National Laboratory, **LA-13709-M**, March 2000.



**Nuclear Engineering Division**

Argonne National Laboratory  
9700 South Cass Avenue, Bldg. 208  
Argonne, IL 60439-4842

[www.anl.gov](http://www.anl.gov)



UChicago ▶  
Argonne<sub>LLC</sub>



A U.S. Department of Energy laboratory managed by UChicago Argonne, LLC